EMERGING TECH CONFERENCE – Edge Intelligence

Volume 01, 2022, Page 192 – 203

Proceedings of Emerging Tech Conference:
Edge Intelligence 2022

Anterior Cruciate Ligament Surgical Reconstruction through Finite Element Analysis

Konstantinos Risvas[a], Dimitar Stanev[b], Athina Kokonozi[a], Konstantinos Moustakas[a],*

[a]*Department of Electrical and Computer Engineering, University of Patras, 25500, Patras, Greece.*
[b]*Institute of Bioengineering, École Polytechnique Fédérale de Lausanne, 1015, Lausanne, Switzerland.*

moustakas@ece.upatras.gr

Abstract

ACL surgery aims to repair or reconstruct the anterior cruciate ligament (ACL) by replacing the injured ligament with a graft. This paper presents an automated workflow for modeling, simulation, and analysis of the ACLR surgery relying on subject-specific data to assist orthopedists in the assessment of surgery options and in the complex task for the identification of the optimal combination of ACLR parameters for each patient, towards optimal ACLR surgery planning. The surgery modeling workflow includes an automatic pipeline which has been developed for modeling surgery parameters based on subject-specific geometries following the MRI segmentation and by considering different surgical techniques. A reference model of the intact knee has been developed and has been validated with data provided by the Open Knee(s) project, for the evaluation of effectiveness of ligament stiffness estimation directly from MRI, while responses with the reference model have been compared through the performance of "what-if" simulations. Results indicate reduced relative knee displacement due to increased graft pretension, correlation of graft radius and tension need to be considered, reduced knee laxity with graft fixation angle of 20°, while single-versus double-bundle techniques demonstrate comparable performance in restraining knee translation. Developed numerical models have been made publicly available.

1. Introduction

An anterior cruciate ligament (ACL) tear is a devastating injury to an athlete and unfortunately is one of the most common knee injuries in athletes involved in rapid deceleration moves. Reconstruction surgery is performed to restore stability to the knee and allow the patient to return to a healthy and active lifestyle. Revision ACL reconstruction is clinically challenging and associated with worse clinical outcomes than primary reconstructions, and a recent systematic review revealed a 13.7 % overall failure rate. Currently in the clinical practice, ACL reconstruction plan is based on options selected from a standard menu and is not driven by the unique characteristics of each patient [1,2,3]. Moreover, graft properties, such as radius, pretension, and harvesting site, are important factors that can potentially affect the results of ACLR and need to be also considered [4,5], while treatment selection is based on subjective clinical experience and not on objective prediction of post-treatment function.

The aim of this paper is to present an automated computational biomechanics pipeline with important steps of ACLR surgery modeling towards realistic subject-specific modeling of all the parameters and aspects of the real-life ACLR. These include the applied surgery technique and the geometric graft characteristics, material properties, pretension, and placement through the bone tunnels. The proposed modelling approach could assist orthopedic surgeons in their decision-making. The proposed modelling framework is materialized by employing open-source software tools.

Nomenclature

ACL Anterior Cruciate Ligament

ACLR Anterior Cruciate Ligament Reconstruction

FE Finite Element

PCA Principal Component Analysis

PCL Posterior Cruciate Ligament

MCL Medial Collateral Ligament

LCL Lateral Collateral Ligament

RM Reference Model

SB Single Bundle

2. Methodology

The pipeline described in this study utilizes MRI data andsubject-specific geometries which feed the development of realistic knee models of the patient, suitable for performing simulations with the FE method. The cruciate and lateral ligaments of the knee are modeled as non-linear one-dimensional springs. Kinematics and dynamics data are input along with the musculoskeletal model to an inverse kinematics problem for the calculation of the muscle forces and reaction forces at the knee joint which constitute the boundary conditions (force - Neumann and displacement - Dirichlet).

“Surgery Modeling” is a tool which has been developed in a Python environment, using Blender software. Blender is an open-source software that supports all steps in creating 3D rendering, including modeling, simulation, rigging, animation, compositing, and motion capture. The “Surgery Modeling” tool is used to model the steps of the ACLR surgery, such as opening the bone channels, creating the graft mesh and placing it in the bone holes.

Moreover, the “FEBioExporter” tool has been developed also in Python and is designed for fast and automated development of the FE models according to the specifications of the free source software FEBio. FEBio is a software tool for nonlinear finite element analysis in biomechanics and biophysics and is specifically focused on solving nonlinear large deformation problems in biomechanics and biophysics [6].

An overview of the proposed workflow is presented in Fig.1.

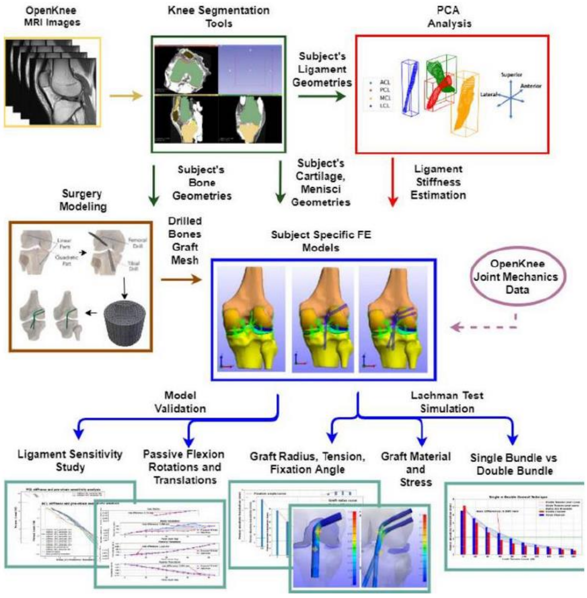

Figure 1: Overview of the proposed workflow [10].

2.1. Cruciate and lateral ligaments modelling

The cruciate and lateral ligaments of the knee are modeled as non-linear one-dimensional springs. The model parameters are determined by the geometric characteristics of the ligaments, as analyzed from medical images and clinical examinations. Methodology includes the following steps:

- Calculation of the average cross-section of the ligaments from their 3D visualization.
- Calculation of the stiffness parameter for each ligament.
- Application of the force-deformation relationship and its appropriate implementation for the development of the models in the selected computing environment.
- Creation of 1D elements (springs) that have bone attachment points resulting from reconstructed ligament and bone geometries.
- Sensitivity analysis based on clinical test results to adjust selected stiffness and pre-distortion values.

The developed software tool automatically implements the above steps. The ligaments are modeled as bundles of non-linear springs with parameters that are adapted to the geometric characteristics of the patient's anatomical structures as reconstructed by the medical images (MRI) and to the results of clinical examinations on the healthy and injured knee. The mathematical model is:

$$F = \begin{cases} 0 & \varepsilon < 0 \\ 0.25k\varepsilon^2/\varepsilon_l & 0 \le \varepsilon \le 2\varepsilon_l \\ k(\varepsilon - \varepsilon_l) & \varepsilon > 2\varepsilon_l \end{cases} \quad (1)$$

F is the spring force, k is the ligament stiffness (N), εl is the linear strain limit with a default value of 0.03, and ε is the strain, as calculated from the spring length value and the zero-strain value L0. Parameter L0 is calculated as follows:

$$L_0 = L_r/(1 + \varepsilon_r) \quad (2)$$

Parameter Lr corresponds to the length of the spring at the initial state of the joint at the beginning of the simulation. The parameter εr corresponds to the pre-existing deformation. The parameter k has SI units measured in Newtons and is calculated as follows:

$$\mathrm{k} = E * A \tag{3}$$

Parameter E refers to the modulus of elasticity of the link (Young's modulus) and is measured in MPa. Parameter A is the cross-section of the link and is measured in mm2. The Young's modulus values are derived from literature and are presented in Table 1.

Joints	Young's modulus (MPa)	Reference Stiffness (N)	Cross Section Reference (mm^2)	Pre-existing Report Distortion
ACL	355	10000	35	0.08
PCL	3014	20100	60	-0.135
MCL	355	8250	24	0.0367
LCL	355	6000	Not Available	-0.073

Table 1. Elasticity measure values

The estimated stiffness value is distributed evenly to each spring by dividing k by the number of ligament springs. The mean cross-section area of each ligament has been estimated from the segmented MRI data. The principal axis of each mesh was found with PCA method. This axis was defined as the normal vector of consecutive planes with an offset of one unit for a range equal to the length of the main diagonal of each mesh bounding box, as shown in Fig.2, where each plane corresponds to a slice of the mesh, and for each slice, the area was estimated. For each ligament, the mean cross-sectional area was the average area of these slices.

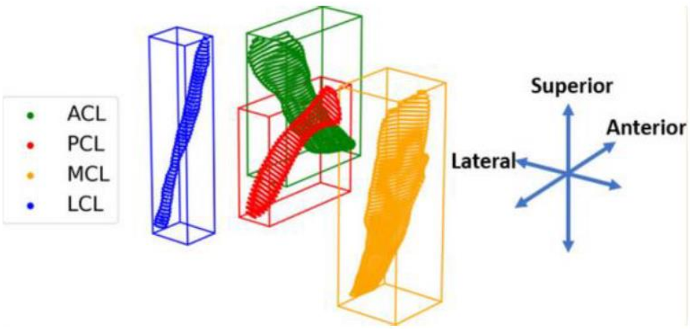

Figure 2: Estimation of ligament stiffness [10]

Joints	Young's modulus (MPa)	Estimated Area (mm)	Reference Area (mm)	Reference Stiffness (N)
ACL	355	35.94	35	10.00
PCL	304	42.12	60	20.10
MCL	355	21.11	24	8250
LCL	355	7.2	N/A	6000

Table 2. Comparison of ligament parameters between estimated and reference literature values

The estimated stiffness and reference prestrain values are used as an initial guess for a sensitivity analysis for the identification of the optimal combination of these parameters. A good match was achieved by varying only the prestrain parameter and keeping the stiffness value unchanged . Thus, different combinations of stiffness and prestrain values might lead to similar responses stressing an inherent uncertainty of the prestrain factor that affects the overall predicted ligament behavior. Aggregated results from the sensitivity analysis with the ten best combinations of stiffness and prestrain values for PCL can be seen in Fig.3. The "s" and "p" denote the stiffness and prestrain percentage change, respectively.

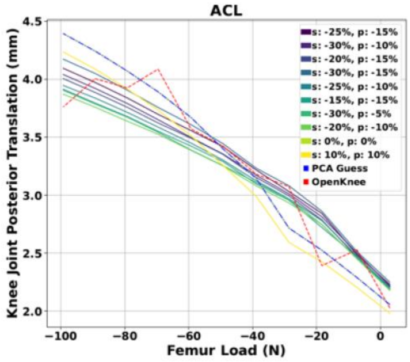

Figure 3: Aggregated results from the sensitivity analysis [10]

2.2. Surgery modelling

Surgery Modeling is used to model the steps of the anterior cruciate reconstruction surgery. The first step is to import the femur and tibia geometries into the Blender software. Then, two landmarks on each bone surface are selected that signify the insertion and exit points of the tunnels. Next step is to create a non-uniform rational B-spline (NURBS) curve to "drill" the bone tunnels and place the graft. The selected landmarks on each bone are the curve's control points. The curve consists of three distinct parts. Inside each bone curve segments are of order 2, and the middle part located in the space between the bones is of order 3, towards smoother curvature that is useful for graft placement. The linear parts of the curve (inside the bones) allow precise placement of the "drills" (cylindrical objects with length slightly larger than the line segment that passes through the pair of the selected landmarks on each bone surface) through the selected landmarks. "Drills" can be attached to the NURBS curve, by applying the Blender curve modifier to the cylindrical meshes. Tunnels are drilled utilizing the Blender's Boolean modifier. A cone object is used for the creation of a "crater" around the entry point of the femoral tunnel, eliminating acute facets on femoral surfaces and avoiding contact breakdown during FE simulations. The graft can be modeled as tetrahedral or hexahedral mesh where a primitive grid is engulfed by a circle mesh with a radius equal to that of the graft. The basic grid is generated by grouping nodes on the circumference of each primitive mesh for the creation of to create quadrilateral faces. Mesh quality is improved by smoothened edges after mesh subdivision. The edges of the refined base grid are then extruded to form base cylindrical meshes with brick-like elements. These cylinders are stacked together to form the final graft mesh. The resolution and length of each cylinder can be easily modified to generate denser meshes in areas of interest to improve numerical accuracy of subsequent FE analyses. Blendbridge software was used to convert the graft surface mesh to a hexahedral volumetric mesh, while the Gmsh software (3D Frontal unstructured algorithm) was applied for graft mesh refinement. Mesh quality test was performed with the use of the meshing quality filters of Paraview software. The facets of the external graft surface have been stored in the form of quartets of node indices to allow automatic selection of contact surfaces pair in the subsequent FE simulation. For automatic selection of surface pairs for contact configuration in the subsequent FE analyses, cylindrical objects have been created which enclose different parts of the graft and bones. These cylinders are also utilized for selecting specific node sets and surface parts of the graft to apply boundary conditions, such as the tension at the bottom surface of the graft.

2.3. FEBioExporter software

The "FEBioExporter" software was developed in Python and allows automatic creation of FE models that can be solved with the available solvers of the FEBio software. Each FEBio model is an .xml structure which consists of several components, which are as follows:

- Meshes representing anatomical structures
- Parameter values for material constitutive equations
- Collision detection models and their parameter values forenforcing contact forces
- Boundary conditions (Forces, Loads, etc.)
- Different types of joints
- Spring (1D) elements
- Solver parameters

System settings are defined in an .xml file and include:

- Patient Reference Code
- Analysis Type: (0) Joint with injured (cut) anterior cruciateligament, (1) joint with healthy anterior cruciate ligament,(2)operated joint with single bone canal in each bone, and(3)operated joint with double bone canal in every bone.
- PS model name code
- Graft material
- Number of graft bonds
- Patella modelling
- Graft tension force
- Graft diameter
- Knee flexion angle during graft placement
- Type of movement
- Method of defining reference systems for joint modelling

The system outputs are as follows:

- FE models of the knee joint, adapted to the settings selected by the user
- Analytics Data based on user choices. These include boneand web nodal displacements and stresses and forces on the tibial cartilages, menisci and graft geometry.
- Graphical representations of results

2.4. Realistic knee musculoskeletal modelling

In this section, we describe the workflow for performing a musculoskeletal analysis of a gait trial. The objective was to acquire suitable boundary conditions for the subsequent FE analyses. The workflow is presented in Fig 5.

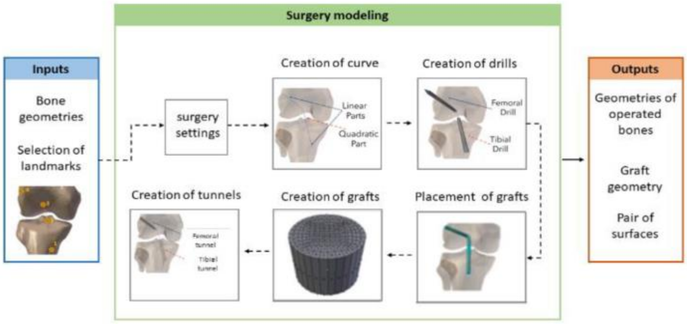

Figure 4: Overview of Surgery modelling workflow

First, the kinematics data and external forces (ground reaction forces) are properly processed to transform them into the format required by OpenSim. The kinematics data and external forces (ground reaction forces) are properly processed to transform them into the format required from OpenSim. The data monitoring through the “Mokka” software, provides useful information such as the names of the experimental reflectors, the definition of the reference system for recording the data, as well as moments of interest, such as the moment contact of the foot with the power floor. Then transformation of data with code based on the OpenSim application programming interface (API) is performed, to export the motions as files in an OpenSim-compatible format (".trc").

Realistic knee models are included in general musculoskeletal models of the whole body (full body models).

The general musculoskeletal model chosen consists of 27 bodies which are connected to each other through 27 joints, which impose 52 degrees of freedom. This model was chosen because both the knee and patella joints allow movement in 6 dimensions (3 degrees of freedom for translation and 3 for rotation). This is achieved by modeling the links as non-linear springs as well as introducing a contact force calculation model

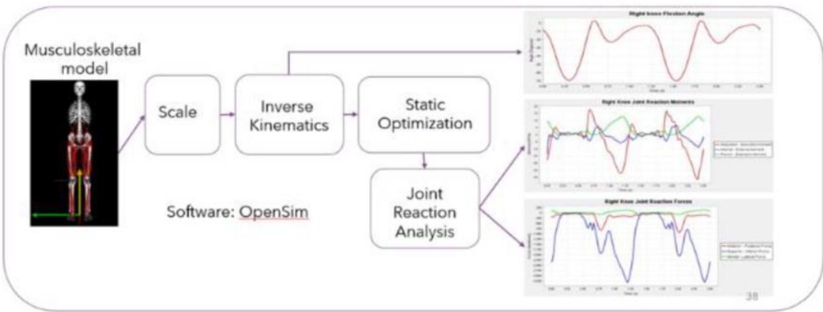

Figure 5: Overview of the process for the extraction of boundary conditions

to calculate the contact forces at the joints. The selection of the generic musculoskeletal model allows us to change the material properties of the ligaments to create customized ligament models as described in section 2.1. In addition, it is necessary to adjust all the anthropometric parameters of the general model for the thorough analysis of the recorded movements. For this purpose, the "Scale Tool" of OpenSim [7] is used. Parallel to the adjustment of the anthropometric data, the displacement of the virtual reflectors on the model is carried out, so that they correspond to the position of the recorded experimental reflectors. Next step includes the use of the individualized musculoskeletal model together with the set of virtual reflectors to calculate the generalized coordinates of the model at each frame of a recorded motion. For this purpose, the "Inverse Kinematics" tool of OpenSim [8] is used.

At the end of the analysis the maximum error for each reflector is checked as well as the square root of the mean square error for all reflectors. Allowed values are between 2-4 cm for the first case and about <2 cm for the second. The knee flexion angle, the first boundary condition for Finite Element analyses, is derived from the Inverse Kinematics analysis. Inverse Kinematics is followed by a Static Optimization analysis to calculate the muscle forces (Static Optimization).

Finally, muscle forces, external forces and model trajectory (time series of generalized coordinates) are used to calculate the reaction forces between the bodies that make up the knee joint [9]. Also, the reference system of the forces is determined, which is very useful for introducing the boundary conditions in the subsequent FE simulations.

3. Results

3.1. Lachman Test

Evaluation of ACLR options such as surgery technique, graft pretension, radius, material, and knee fixation angle, has been performed with the use of Lachman test simulation. To this end multiple FE models have been developed, and their performance was compared to that of the validated RM model. Clinical data were used to achieve the comparison. These data describe relative displacements between the femur and tibia during the Lachman Test clinical examination, for both the healthy and the injured knee. Therefore, each cruciate reconstruction FE model was compared to the healthy knee.

Effect of graft radius and pretension level. For each value of the graft radius between 1.5 mm and 5.5 mm with a step of 0.5 mm 9 models were created. Also, 10 models were created with a graft radius of 4 mm and tension values from 0 - 180 Newtons

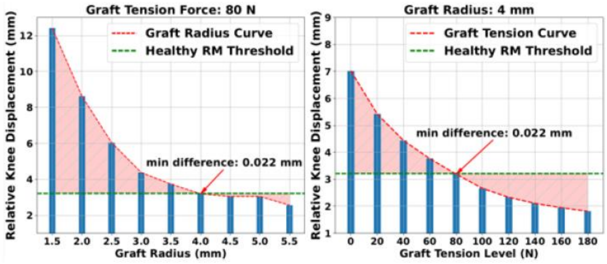

Figure 6: Overview of the process for the extraction of boundary conditions

in steps of 20 Newtons. For each model the boundary conditions were applied, and the simulations were performed. At the end of each simulation, the displacement of the center of mass of the femur was measured. The comparative results for the analysis of the effect of the radius size on the instability confinement are shown in the left part of Fig.6.We observe that an increase in the radius of the graft causes an exponential decrease in displacement. Compared to the response of the Reference Model, which is represented by the straight green dashed line, we observe that a radius value close to 4 mm is the most appropriate choice. In addition, the right part of Fig.6 shows the results for the graft tension. Similarly, a non-linear decrease in displacement with increasing voltage value is observed. Also, a stress value of 80 Newtons emerges as the optimal choice compared to the response of the healthy joint model under the same boundary conditions.

Effect of graft tissue choice. Three different graft materials

Semitendinosus				Patellar tendon				Gracilis			
Radius (mm)	Pretension (N)	Error (mm)	Stress (MPa)	Radius (mm)	Pretension (N)	Error (mm)	Stress (MPa)	Radius (mm)	Pretension (N)	Error (mm)	Stress (MPa)
3	120	0.116	31.2	4	80	0.016	23.8	2.5	160	0.012	54.6
4	80	0.122	22.6	2.5	160	0.055	53.7	3.5	80	0.046	33.4
3.5	100	0.186	31.7	3	120	0.067	32.9	4	80	0.061	24.2
5.5	60	0.200	18.6	5.5	60	0.223	22.7	3	120	0.127	33.4
2.5	180	0.257	52.7	3.5	80	0.111	32.7	5.5	60	0.132	23.1

Table 3. Qualitative results depicting the five best models and parameter combinations for each of the three grafts [10].

Corresponding to the semitendinosus, patellar tendon, and gracilis harvest sites have been analyzed, to examine also changes in the tissue response for different combinations of pretension and graft radius levels. Results showed that all three grafts exhibit similar behavior in the range of 60–100 N and radii between 3.5 and 5 mm, and that the most effective combination in terms of minimizing knee laxity is a gracilis graft with a radius of 2.5 mm and a pretension load of 160 N. A small radius requires excessive graft pretension, as observed by this combination and all other pairs with radii 2.5 mm. A graft with a 4 mm radius and 80 N pretension demonstrates a consistent performance, with all three materials. In general, grafts with ranges of radius between 3 and 4 mm and pretension between 80 and 120 N perform adequately in restraining relative knee translation.

Effect of graft fixation angle. A semitendinosus graft of 4 mm radius and an applied pretension of 80 N was used. The increase of the knee flexion angle above 30∘ when fixing the graft through the bone tunnels leads to increased relative knee displacement. Fixation angle curve between 15∘ and 20∘ produces the closest performance to that of the healthy RM, with an absolute difference in relative knee displacement of approximately 0.07 mm. For the range between full extension and 10∘ the knee is over-constrained.

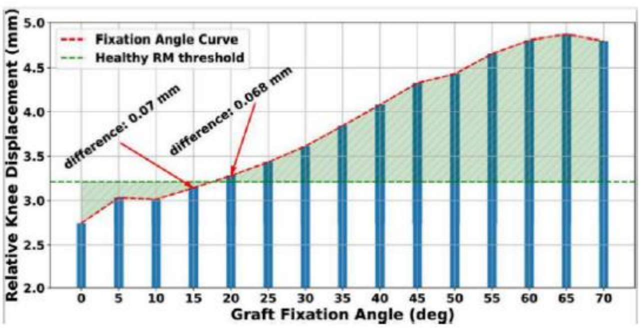

Figure 7: Effect of graft fixation angle on relative knee displacement [10].

Single channel versus double channel. For the comparison study, a single graft with a radius of 5 mm for the SB case and two grafts of radii 2.5 mm for the DB approach were used. The best performance for SB is for graft pretension of 80 N with 0.17 mm of absolute difference in relative knee displacement. Best performance for DB was observed for a pretension of 60N applied on both grafts. According to results, both techniques demonstrate a comparable performance.

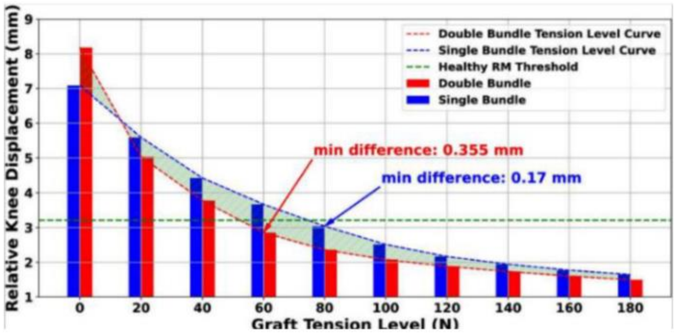

Figure 8: Results for comparing the SB and DB techniques [10].

3.2. Gait Analysis

This section includes the boundary conditions and results for a gait simulation using a single bone hole PS model. A single beam model with a radius of 3 mm and three different stress values of 80, 120 and 160 Newtons was used for the analysis. Also, the geometries for the double bone hole models were created using the 'Surgery Modeling' tool. For this purpose, the procedure described in section 2.2 was followed, for each of the two bone canals and therefore the two grafts. The extraction of boundary conditions follows the workflow presented in section 2.4. These are the flexion angle and knee joint reaction forces that occur between the femur and tibia during musculoskeletal analysis using OpenSim Biomechanics software. Rotational forces (torques) data were converted to Newtons * mm. The final boundary conditions applied to the PS models are as follows:

- Bending angle up to 20 degrees
- Pressure force on the bottom surface of the graft to simulate the application of stress to the graft. The pressure load is equal to P=F / A , where F is the desired stress and A is the graft cross-section
- Knee back to full extension
- Description of forces in the following joint degrees of freedom: i) Force in the vertical axis, ii) Torque around the front axle (input - output torque).

The following constraints are defined: limitations to all grades for the tibia, limitation in internal-external rotation, anterior-posterior displacement for the femur.

Graft Tension Effect: we performed simulations to study the effect of graft tension on contact stresses in tibial cartilage and von Mises forces in menisci. Fig.9 shows the results for the contact pressures in the tibial cartilages (left: external lateral cartilage, right: medial lateral cartilage) for different graft stresses. An increase in pressure on the lateral cartilage is observed with increasing stress on the graft.

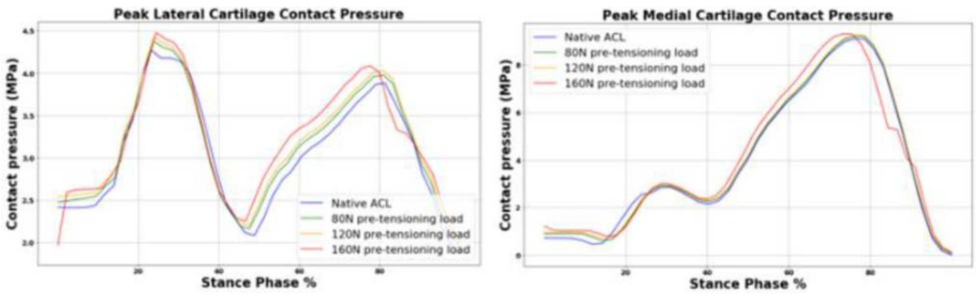

Figure 9: Contact pressure forces on the outer (left) and inner (right) tibial cartilage for three different values of graft stress

Effect of Single or Double Tunnel: simulations have been performed to study the effect of choosing between single and double bone tunnel surgery on the contact stresses in the tibial cartilages and the von Mises forces in the menisci. For the double-hole PS models, three different stress values of 80, 120, and 160 Newtons were applied (Fig.10). Increased in forces is observed with increased graft stress in the double bundle models, which is greater in the case of the outer meniscus. The forces are smaller compared to the reference model and the single bone hole model. In the case of the medial meniscus the forces for the double bone hole models are greater in the first phase of the single support period than in the middle and second phases.

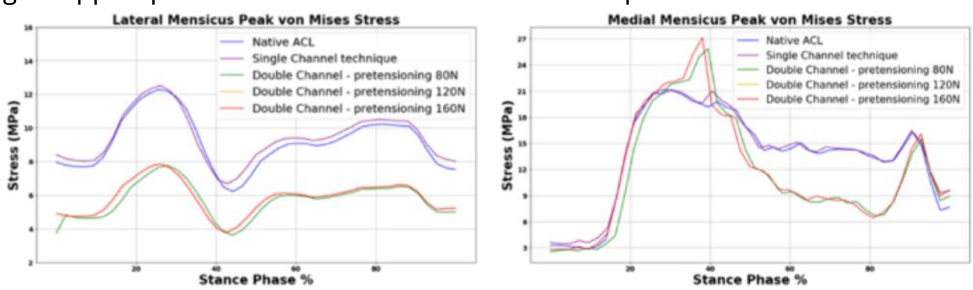

Figure 10: Von Mises forces on the outer (left) and inner (right) meniscus for three different graft stress values

Discussion

In this paper authors presented an automated workflow for modelling, simulation, and analysis of the ACLR surgery based on subject-specific data. The pipeline can be used to assess the majority of surgery parameters in a simulation manner, using open-source tools. The described models provide outputs comparable to experimental data used for validation and predictions proposed by comparative studies. The current study does not include dynamic movements for the investigation of long-term effects of the ACLR parameters, or conditions with increased potential risk of graft rupture and ACL surgery revision. Future research could focus on modelling the patellofemoral joint structures and on investigating the contribution from the muscles that span the knee joint. Results indicate that the proposed workflow could be used for surgery planning and support efforts towards the identification of optimal combination of ACLR parameters for a particular subject.

Acknowledgements

This research has been co-financed by the European Regional Development Fund of the European Union and Greek national funds through the Operational Program Competitiveness, Entrepreneurship, and Innovation, under the call RESEARCH–CREATE–INNOVATE (project code: T1EDK-04234).

References

[1]. Kilinc, B. et al. Transtibial vs anatomical single bundle technique for anterior cruciate ligament reconstruction: A retrospective cohort study. Int. J. Surg. (London, England) 29, 62–69. https://doi.org/10.1016/j.ijsu.2016.03.025 (2016).

[2]. Lim, H., Yoon, Y.-C., Wang, J.-H. & Bae, J.-H. Anatomical versus non-anatomical single bundle anterior cruciate ligament reconstruction: A cadaveric study of comparison of knee stability. Clin. Orthop. Surg. 4, 249–55. https://doi.org/10.4055/cios.2012.4.4.249 (2012).

[3]. Bedi, A. et al. Transtibial versus anteromedial portal reaming in anterior cruciate ligament reconstruction: An anatomic and biomechanical evaluation of surgical technique. Arthrosc. J. Arthrosc. Relat. Surg. 27, 380–390. https://doi.org/10.1016/j.arthro.2010.07.018 (2011).

[4]. Järvelä, S., Kiekara, T., Suomalainen, P. & Järvelä, T. Double-bundle versus single-bundle anterior cruciate ligament reconstruction: A prospective randomized study with 10-year results. Am. J. Sports Med. 45, 363546517712231. https://doi.org/10.1177/0363546517712231 (2017).

[5]. Jaglowski, J. R., Williams, B. T., Turnbull, T. L., LaPrade, R. F. & Wijdicks, C. A. High-load preconditioning of soft tissue grafts: An in vitro biomechanical bovine tendon model. Knee Surg. Sports Traumatol. Arthrosc. Off. J. ESSKA 24, 895–902. https://doi.org/10.1007/s00167-014-3410-x (2016).

[6]. https://febio.org/

[7]. https://simtk-confluence.stanford.edu:8443/display/OpenSim/Scaling

[8]. https://simtk- confluence.stanford.edu:8443/display/OpenSim/Inverse+Kinematics.

[9]. https://simtk-confluence.stanford.edu:8443/display/OpenSim/Joint+Reactions+Analysi

[10]. K. Risvas, D. Stanev, L. Benos, K. Filip, D. Tsaopoulos και K. Moustakas, «Evaluation of anterior cruciate ligament surgical reconstruction through finite element analysis,» Scientific Reports, 12, 8044, 16 May 2022.